

**AD-A265 037**



(2)

**OFFICE OF NAVAL RESEARCH**

**GRANT N00014-89-J-1178**

**R&T CODE 413Q001-05**

**TECHNICAL REPORT NO. #58**

**AN ELLIPSOMETRY INVESTIGATION OF NUCLEATION AND GROWTH OF  
ELECTRON CYCLOTRON RESONANCE PLASMA DEPOSITED SILICON FILMS**

**M. Li, Y.Z. Hu, J. Wall, K. Conrad, and E.A. Irene**  
**Department of Chemistry**  
**University of North Carolina at Chapel Hill**  
**Chapel Hill, NC 27599-3290**

**Submitted to:**

**Journal of Vacuum Science and Technology**

**Reproduction in whole or in part is permitted for any purpose of the United States  
Government.**

**This document has been approved for public release and sale; its distribution is  
unlimited.**

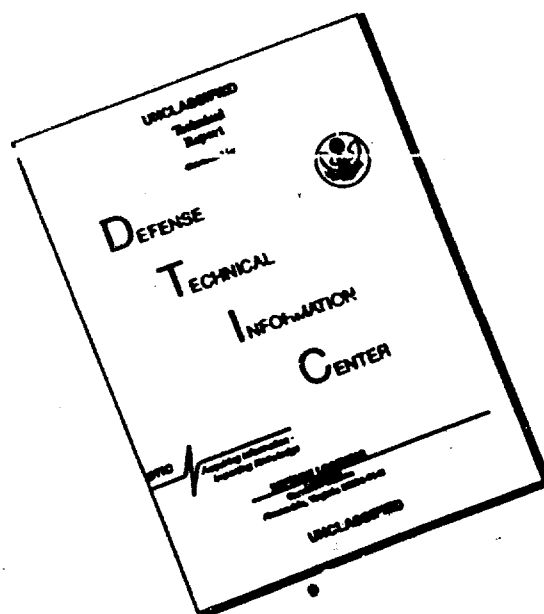
**DTIC**  
**S ELECTE D**  
**JUN 01 1993**  
**B**

**93 5 28 014**

**93-12131**

1708

# DISCLAIMER NOTICE



THIS DOCUMENT IS BEST QUALITY AVAILABLE. THE COPY FURNISHED TO DTIC CONTAINED A SIGNIFICANT NUMBER OF PAGES WHICH DO NOT REPRODUCE LEGIBLY.

# REPORT DOCUMENTATION PAGE

Form Approved  
OMB No 0704 0188

Public reporting burden for this collection of information is estimated to average 1 hour per response, including the time for reviewing instructions, searching existing data sources, gathering and maintaining the data needed, and completing and reviewing the collection of information. Send comments regarding this burden estimate or any other aspect of this collection of information, including suggestions for reducing this burden, to Washington Headquarters Services, Directorate for Information Operations and Reports, 1215 Jefferson Davis Highway, Suite 1204, Arlington, VA 22202-4302, and to the Office of Management and Budget, Paperwork Reduction Project (0704-0188), Washington, DC 20503.

1. AGENCY USE ONLY (Leave blank)		2. REPORT DATE 5/4/93		3. REPORT TYPE AND DATES COVERED	
4. TITLE AND SUBTITLE An Ellipsometry Investigation of Nucleation and Growth of Electron Cyclotron Resonance Plasma Deposited Silicon Films.				5. FUNDING NUMBERS #N00014-89-J-1178	
6. AUTHOR(S) M. Li, Y.Z. Hu, J. Wall, K. Conrad, and E.A. Irene					
7. PERFORMING ORGANIZATION NAME(S) AND ADDRESS(ES) The University of North Carolina Chemistry Department CB #3290 Venable Hall Chapel Hill, NC 27599-3290				8. PERFORMING ORGANIZATION REPORT NUMBER  Technical Report #58	
9. SPONSORING / MONITORING AGENCY NAME(S) AND ADDRESS(ES) Office of Naval Research 800 N. Quincy Street Arlington, VA 22217-5000				10. SPONSORING / MONITORING AGENCY REPORT NUMBER	
11. SUPPLEMENTARY NOTES None					
12a. DISTRIBUTION / AVAILABILITY STATEMENT This document has been approved for public release and sale, distribution of this document is unlimited.				12b. DISTRIBUTION CODE	
13. ABSTRACT (Maximum 200 words) The nucleation and initial growth of Si films is fundamental to the understanding and control of rapid thermal CVD, RTCVD, and plasma enhanced CVD, PECVD processes. Herein we report on the nucleation and growth of Si deposited on oxidized silicon wafers by ECR PECVD in 600-700 °C temperature range, under low pressures, and using both in situ spectroscopic ellipsometry (SE) and single wavelength real-time ellipsometry. An island growth and coalescence model is used to interpret the real-time ellipsometry data. Initial nuclei distance and growth parameters are derived. Atomic Force Microscopy (AFM) was used to observe the early stage of nucleation. In situ spectroscopic ellipsometry is used to measure the final Si film thicknesses and optical properties. The structure of the deposited crystalline Si films were characterized by XTEM.					
14. SUBJECT TERMS Cyclotron Resonance Plasma				15. NUMBER OF PAGES	
				16. PRICE CODE	
17. SECURITY CLASSIFICATION OF REPORT Unclassified	18. SECURITY CLASSIFICATION OF THIS PAGE Unclassified	19. SECURITY CLASSIFICATION OF ABSTRACT Unclassified	20. LIMITATION OF ABSTRACT		

**An Ellipsometry Investigation of Nucleation and Growth of  
Electron Cyclotron Resonance Plasma Deposited Silicon Films**

M. Li, Y.Z. Hu, J. Wall, K. Conrad and E.A. Irene  
Department of Chemistry, The University of North Carolina  
Chapel Hill, NC 27599-3290

**Abstract**

The nucleation and initial growth of Si films is fundamental to the understanding and control of rapid thermal CVD, RTCVD, and plasma enhanced CVD, PECVD processes. Herein we report on the nucleation and growth of Si deposited on oxidized silicon wafers by ECR PECVD in 600-700 °C temperature range, under low pressures, and using both in situ spectroscopic ellipsometry(SE) and single wavelength real-time ellipsometry. An island growth and coalescence model is used to interpret the real-time ellipsometry data. Initial nuclei distance and growth parameters are derived. Atomic Force Microscopy(AFM) was used to observe the early stage of nucleation. In situ spectroscopic ellipsometry is used to measure the final Si film thicknesses and optical properties. The structure of the deposited crystalline Si films were characterized by XTEM.

**Introduction**

The study of Si film nucleation and growth has been ongoing for decades<sup>1-9</sup>. Ellipsometry techniques used in various environments such as low pressure and plasma enhanced chemical vapor deposition, LPCVD and PECVD, respectively, have been extensively utilized to study the Si nucleation and growth behavior, particularly for amorphous silicon(a-Si) for photoelectronics device applications<sup>5-8</sup>. Hottier and Cadoret<sup>9</sup> used single wavelength ellipsometry to study polycrystalline Si(Poly-Si) nucleation on Si<sub>3</sub>N<sub>4</sub> a decade ago. The recent trend toward selective deposition for integrated circuit, IC, applications with Poly-Si's importance in the IC field, has refocused attention on the area of Si film nucleation and growth. Our approach is to use in-situ ellipsometry to examine Si film nucleation resulting from rapid thermal, RT, and electron cyclotron resonance, ECR, plasma processes with potential application to Si selective epitaxy growth(SEG)<sup>10</sup>.

Both RT and ECR plasma CVD have been shown to be useful in SEG applications<sup>11-13</sup>. RTCVD employs low thermal exposure, while ECR is preferred for large area uniformity and low temperature deposition. In this work, we show Si film nucleation and growth in ECR plasma system. The work on RTCVD will be reported separately.

**Experimental**

Si films were deposited onto n-type, <100> Si crystal wafers which were thermally

oxidized to have about 24 nm thick SiO<sub>2</sub>. The temperatures and gas flow rates were varied and the effect on nucleation and growth were monitored.

The details of the ECR plasma and ellipsometer systems can be found elsewhere<sup>14</sup>. The samples were first heated to desired temperatures by a lamp heater behind wafer, and deposition was followed at 400 W and 2.45 GHz microwave power, in an Ar plasma under ECR conditions with +5 volt substrate bias. For Si films a 3% SiH<sub>4</sub> with Ar gas mixture was used.

A rotating analyzer spectroscopic ellipsometer, with an angle of incidence of 70°, was used in-situ to monitor the film formation. Spectroscopic ellipsometry, SE, data was used for optical modeling and single wavelength ellipsometry at a selected wavelength for real-time measurements. Our real-time ellipsometry was carried out at a wavelength of 365 nm (3.4 eV), with a minimum data acquisition time of ~ 1 second. The SE scans were made in the photon energy range from 2.5 to 5.0 eV.

In modeling Si nucleation, the ellipsometric  $\Psi$  and  $\Delta$  data are compared to the calculated  $\Psi$  and  $\Delta$  as obtained from models to be discussed below. The nuclei are assumed to grow in a hexagonal network. Upon coalescence of the nuclei, voids may be left under the film at the interface, or on top of the film to represent surface roughness or both. In this approach, a continuous one-film model is used, with film thickness identical to the nuclei height and the film properties constructed from that of bulk Si and voids (air) by using the Bruggemann effective medium approximation (BEMA)<sup>15</sup> as:

$$f_v \frac{N_{Si}^2 - N^2}{N_{Si}^2 + 2N^2} + (1 - f_v) \frac{1 - N^2}{1 + 2N^2} = 0$$

where  $f_v$  is the volume fraction of Si in the film calculated based on the geometric model,  $N_{Si}$  and  $N$  are the complex refractive indices for Si and the film, respectively. The optical data for Si at high temperature was obtained from our SE measurements of a-Si and c-Si at temperature. In order to prevent crystallization of a-Si, lower temperatures (~ 600 °C) were used.

In optical modeling by SE,  $\Psi$  and  $\Delta$  were converted to the pseudo-dielectric function  $\langle \epsilon \rangle$ ,

$$\langle \epsilon \rangle = \sin^2 \phi \left[ 1 + \left( \frac{1 - \rho}{1 + \rho} \right)^2 \tan^2 \phi \right]$$

where  $\rho = \tan \Psi e^{i\Delta}$ ,  $\phi$  is the angle of incidence. A non-linear curve fitting routine was used to fit the experimental data both in SE and real-time ellipsometry.

## Results and Discussion

### 1. The Nature of the ECR Plasma Deposited Si Films

In order to construct a reasonable optical model, the Si films need to be characterized. The deposited Si films were characterized by spectroscopic ellipsometry, SE, and cross sectional TEM, XTEM. Fig. 1a illustrates the imaginary part,  $\langle \epsilon_2 \rangle$ , of the pseudo-dielectric function,  $\langle \epsilon \rangle$ , spectra for ECR PECVD Si films at sample temperatures of 605 to 700 °C. All the spectra show features of c-Si which has peaks located at photon energy of 3.4 and

Availability Codes	
Dist	Avail and/or Special
A-1	

4.2 eV(dashed spectrum). Shown in Fig. 1b is the calculated  $\langle \epsilon \rangle$  spectra(solid lines) as obtained from the optical model shown in Fig. 2a, for a Si film grown at 630 °C. The Si film is dominated by c-Si, and a-Si. On top of the Si film is a roughness layer which is found to be necessary for better data fitting. The roughness layer is considered to be a mixture of a-Si, voids and SiO<sub>2</sub>. Table I compares all samples in the roughness layer thickness and Si film compositions for ECR PECVD deposited Si films.

The XTEM result in Fig. 2b reveals that the deposited Si film is Poly-Si which has columnar structure and has a thickness comparable to the calculated result from SE as shown in Fig. 2a.

The optical model is consistent with XTEM, but the a-Si fraction obtained from the model must be due to the large amount of grain boundaries. Over all, the ECR deposited films are uniform, with a thin surface roughness layer, and have the characteristics of c-Si. It is also noticed that the volume fraction of voids in the Poly-Si film increased significantly from 7% to 11% with a deposition temperature rise from 620 °C to 630 °C.

## 2. Nucleation Models

Si growth on an amorphous substrate follows an incubation period, during which Si atom nuclei form and coalesce<sup>1</sup>. These events are influenced by a number of factors, such as temperature, Si precursor concentration, and substrate condition, etc. In general, the formation of a film follows three modes of growth:<sup>16</sup> 1) layer-by-layer growth, where nucleation is kinetically unimportant. 2) Volmer-Weber nucleation, where individual island nuclei form and coalesce, and 3) Stranski-Krastanov growth, in which a few monolayers of film are first formed, and then island nucleation follows. Our later discussion of the experimental data will only consider the first two models, since we didn't observe Stranski-Krastanov growth.

To represent nucleation, we use two extreme geometric models: 1) hemispherical nucleation model, and 2) cylindrical(or disk-like) nucleation model. The hemispherical model is adequate for a-Si:H on an amorphous substrate such as SiO<sub>2</sub> and on some metals such as Mo, while the cylindrical model holds for a-Si:H on c-Si, and  $\mu$ c-Si on c-Si<sup>5-8</sup>. The use of a hemispherical cap on top of the cylindrical disk may better represent surface roughness<sup>6</sup>. Fig. 3 shows calculated  $\Psi$ ,  $\Delta$  trajectories for Si nucleation on SiO<sub>2</sub> for the two models. For both models  $D$  is the distance between the nuclei assuming a hexagonal nuclei array, and  $D=0$  simulates layer-by-layer growth and is shown as the dashed line in Fig. 3a and b. Fig. 3a for hemispherical nucleation shows that the radius of the nuclei increases continuously until the hemispheres come into contact. The positions in the  $\Psi$ ,  $\Delta$  plane where the nuclei come into contact are marked by squares. In Fig. 3b which is for cylindrical nucleation, the nuclei grow to form columnar structures until contact, and then grow vertically. In this model, the growth ratio,  $\kappa$ , which is defined as the growth rate in the plane parallel to the surface to the out of plane or vertical growth direction, is assumed to be one<sup>6</sup>. Both simulations assume that surface roughness evolves from the initial nucleation mode and remains unchanged after coalescence. A constant growth rate and film refractive index( $N=5.0-2.8i$ ) are assumed in both models and shown as the solid lines. Other values of  $\kappa$  are also shown in Fig. 3b as dashed lines, and  $\kappa$  has a significant effect on nucleation. The difference between these two models is mainly in the final film surface morphology, one

with hemispherical shape and another with disk shape. The treatment of coalescence for cylindrical nucleation is more complicated than for hemispherical model, in that a cone type model was found to be necessary to interpret the data for  $\mu\text{-Si}$  growth on  $\text{c-Si}$ <sup>6</sup>.

From the simulation, island growth can be clearly distinguished from the layer-by-layer growth from the initial slope of the  $\Psi$ ,  $\Delta$  trajectory. Also, the ellipsometry trajectory provides information about the Si cluster density, as calculated from the initial nuclei distance and geometric distribution of the nucleus at the very early stage of film growth<sup>6</sup>. The evolution of  $\Psi$  and  $\Delta$ , and the endpoint provides details about film coalescence and surface roughness.

### 3. AFM Images of Initial Nucleation

As shown above, the nucleation of Si can be evaluated by observing real-time ellipsometric data and our results will be shown and discussed below. However, it is useful to use atomic force microscopy, AFM, to image the  $\Psi$ ,  $\Delta$  region which shows nuclei to be present, i.e. prior to coalescence. Fig. 4a shows an AFM image of the deposited Si film for a measured  $\Delta$  decrease of  $\sim 7^\circ$ , as is shown in Fig. 4b. Si islands are observed with approximate height of 5 nm and a separation of approximately 30 nm. We also found that for different temperatures which will be shown to significantly influence Si film growth, the AFM images for the early stages of film nucleation show similar morphologies.

### 4. ECR PECVD of Poly-Si

Using the optical models and information from SE, XTEM and AFM presented above, we follow the real time evolution of Si nucleation on  $\text{SiO}_2$  using single wavelength ellipsometry.

#### a) Temperature effect

Fig. 5a shows data of real-time  $\Psi$ ,  $\Delta$  trajectories for five different temperatures with 0.06 min time interval between data points. The growth at lower temperatures (605 °C and 620 °C) follow a similar lobe shaped contour, with  $\Delta$  decreasing by about  $7^\circ$ , and  $\Psi$  increasing by about  $0.5^\circ$  in the initial region. The  $\Psi$ ,  $\Delta$  trajectory at these temperatures looks like that for a-Si grown at temperature below 570 °C (which is not included in the figure). The nucleation and growth at temperatures above 630 °C is significantly different. At temperatures around 630 °C, a larger lobe shape results from nucleation. After coalescence,  $\Psi$ ,  $\Delta$  return to the opaque condition of  $\Psi = 24^\circ$ ,  $\Delta = 145^\circ$ , which is the same endpoint for the two lower temperature data sets. The nucleation and growth at 650 °C and 700 °C show similar initial nucleation but a different later stage of growth.

Fig. 6a shows  $\Delta$  versus  $\Psi$  data for 620 °C. The solid line is a best-fit curve calculated from the cylindrical model using a refractive index  $N = 4.4 - i3.0$ . As mentioned earlier, the a-Si and c-Si data at high temperatures are measured by SE. However, both a-Si and c-Si have refractive indices that depend on temperature, and the a-Si index is dependent on the specific growth procedure. Also, it is never easy to decide whether the a-Si or the c-Si index is appropriate for modeling. For this reason, the refractive index chosen in the modeling is from our measurement, although the final value was deduced from curve fitting.

Also shown for comparison is the homogeneous layer-by-layer growth model which is seen to be different from the experimental result. The cylindrical island nucleation model fits the

data with an island distance of 30 nm as determined by AFM (Fig. 4a) as a fixed parameter, and with a growth ratio,  $\kappa=2$ . A schematic of this model is shown in the insert of Fig. 6a. However, the hemispherical geometry model is also adequate for data fitting, but it yields an island distance,  $D$ , of about 5 nm which doesn't agree with the AFM measurement. We expect that in this temperature range, the Si precursors are more likely absorbed on the surface, so that Si nuclei are able to contact to form a continuous film. This is the Kaschiev model<sup>17</sup> by which the deposition is accomplished by the formation of two-dimensional critical nuclei, followed by lateral extension. Upon coalescence of the Si nuclei, a continuous film is formed which progresses in thickness with a thin roughness layer on top.

As seen in Fig. 5a, the nucleation and growth behavior at 630 °C is different. From the  $\Psi$ ,  $\Delta$  plot, Fig. 6b shows the large change of both  $\Psi$  and  $\Delta$  in the initial region. This corresponds to nucleation with a large  $D$  or sparse nucleation. However, neither the hemispherical nor the cylindrical type model fits the data very well over the range of growth. Three dashed lines in the figure are for the hemispherical model with  $D=8$ , 20, and 30 nm, respectively. A cone-like model, which is the solid line in Fig. 6b is necessary to fit the initial part of the data. In this model, the Si nuclei grow with a growth ratio of 1.3. The nuclei grow faster out of plane prior to contact. An angle,  $\theta$ , is introduced to simulate the conical shape of the nuclei and this angle along with the contact factor  $S$ , the initial nuclei width divided by  $D$ , determine whether nuclei coalesce to form a continuous film. Also, we did not observe a cusp feature which indicates surface relaxation<sup>5</sup>. We note that this feature was observed in our recent RTCVD measurements, but it will not be reported here. We expect that the Si nuclei upon coalescence form a continuous film leaving a surface roughness layer as indicated in Fig. 6b using the hemispherical model fitted with  $D=8$  nm, at the later stage of growth.

We emphasize that our approach for the ECR plasma Si nucleation and growth model agrees with an earlier morphological study of Poly-Si growth at low and high temperatures<sup>1</sup>, and theoretical calculations of surface morphology in CVD for the slow and fast kinetics<sup>18</sup>.

For higher temperatures of 650 and 700 °C, the initial nucleation can be similarly fitted to the cone model and Table II list some fitting parameters. However, using our current model we are not able to fit the later stage of growth. From our SE results for these temperatures, we see that the surfaces are rougher and there are larger void fractions in the Poly-Si film. We expect that at these temperatures, the Poly-Si roughness dominates the optical measurement.

#### b) SiH<sub>4</sub>/Ar flow rate

Fig. 5b is for the  $\Psi$ ,  $\Delta$  data for different SiH<sub>4</sub>(3%) flow rates at 700 °C. In all experiments, Ar was kept at same flow rate of 20 sccm and the total pressure was nearly constant. We see at this high temperature that clear features of nucleation were observed which varied with SiH<sub>4</sub> flow rate. The initial data were fitted using the same model as in Fig. 6b with fitting parameters listed in Table IIb.

In the model,  $\theta=0$  indicates that the film barely coalesces to form a continuous film. When SiH<sub>4</sub> flow rate is low, Si atoms are more likely to form isolated nuclei or crystal facets. Also, it is interesting to observe that increasing the flow rate does not change this behavior very much. From another point of view, whether Si nucleation will form a continuous film



or not depends mainly on the surface temperature in our range of experimental conditions.

### Conclusions

The nucleation and growth behavior of Poly-Si in ECR PECVD have been studied using XTEM, AFM, SE and single wavelength real-time ellipsometry. The data for nucleation and growth of Poly-Si from  $\text{SiH}_4$  on oxidized silicon substrates, can be interpreted using an island nucleation model, where cylindrical type islands with an initial spacing in agreement with AFM measurements. The initial spacing,  $D$ , does not depend strongly on temperature, and is around 30 nm, which is larger than that (10 nm) for a-Si growth as reported by other authors<sup>9</sup>. Complete coalescence is observed for ECR PECVD at lower temperatures. At higher temperatures, a cone-like model has to be used to fit the data.

We have shown how the wafer temperature and gas flow rate affect nucleation and growth. Higher temperatures seem to increase the surface roughness as well as increase the growth rate, while the low  $\text{SiH}_4$  flow rates barely results in continuous films.

### Acknowledgment

The authors thank Ms. L. Martin and Dr. D. Maher (NCSU) for XTEM measurements. One of us (ML) is grateful for a graduate fellowship from the NSF supported Engineering Research Center at North Carolina State University. This research is supported by the NSF Engineering Research Center at North Carolina State University.

### References

1. J. Bloem, J. Crystal Growth, **50**, 581(1980).
2. W.A.P. Claassen and J. Bloem, J. electrochem. Soc., Vol. **127**(1), 194(1980).
3. M.S. Abrahams, C.J. Buicchi, R.T. Smith, J.F. Corboy, Jr., J. Blanc and G.W. Cullen, J. Appl. Phys., **47**(12), 5139(1976).
4. N. Matsuo, H. Ogawa, T. Kouzaki and S. Okada, Appl. Phys. Lett., **60**(21), 2607(1992).
5. R.W. Collins and J.M. Cavese, J. Non-Crystalline Solids, **97&98**, 269(1987).
6. R.W. Collins and B.Y. Yang, J. Vac. Sci. Technol., **B Vol. 7**(5), 1155(1989).
7. A.M. Antoine, B. Drevillon and P.P. Cabarrocas, J. Appl. Phys., **61**(7), 2501(1987).
8. A.M. Antoine, B. Drevillon, J. Appl. Phys., **63**(2), 360(1988).
9. F. Hottier and R. Cadoret, J. Crystal Growth, **56**, 304(1982).
10. J. O. Borland and C.I. Drowley, Solid State Technology, **August**, 141(1985).
11. T.Y. Hsieh, K.H. Jung, D.L. Kwong, T.H. Koschmiederand and J.C. Thompson, J. Electrochem. Soc., Vol. **139**(7), 1971(1992).
12. H. Yamada and Y. Torii, J. Appl. Phys., **64**(2), 702(1988).
13. N. Kasai and N. Endo, J. Electrochem. Soc., Vol. **139**(7), 1983(1992).
14. J. Andrews, Y.Z. Hu and E.A. Irene, SPIE Proceeding **1188**, 162(1989).
15. D.A.G. Bruggemann, Ann. Phys., (Leipzig) **24**, 636(1935).
16. J.A. Venables, G.D.T. Spiller and M. Hanbuchen, Rep. Prog. Phys., Vol. **47**, 399(1984).
17. D. Kashchiev, J. Crystal Growth, **40**, 29(1977).
18. G.S. Bales, A.C. Redfield and A. Zangwill, Phys. Rev. Lett., **62**(7), 776(1989).

## Table Captions

**Table I.** Comparison of ECR PECVD Si films composition as a function of temperature.

**Table II.** Comparison of the fitting parameters for the cone-like cylindrical model for different temperatures and gas flow rates for ECR PECVD Poly-Si.

## Figure Captions

**Fig. 1.** Pseudodielectric function,  $\langle \epsilon \rangle$  versus photon energy spectra for ECR PECVD Poly-Si films: **a)** experimental data for different temperatures; **b)** calculated spectra using the optical model shown in Fig. 2b. Also included as dashed lines is the spectra for c-Si.

**Fig. 2. a)** A schematic optical model; **b)** Cross sectional TEM of a deposited Poly-Si film at 630 °C.

**Fig. 3.**  $\Psi$ ,  $\Delta$  simulation data assuming a hemispherical nucleation model (**a**) and cylindrical model (**b**). The island distance,  $D$ , is varied from 0 nm to 30 nm. Coalescence of nuclei is marked by squares.

**Fig. 4. a)** AFM image of initial nucleation stage of ECR PECVD Si nuclei on  $\text{SiO}_2$  surface; **b)** a corresponding  $\Psi$ ,  $\Delta$  plot showing the position (marked by a square) where AFM image was taken.

**Fig. 5.** Real-time single wavelength  $\Psi$ ,  $\Delta$  data as function of wafer temperature (**a**); as function of  $\text{SiH}_4$  flow rate at 700 °C (**b**), for ECR PECVD of Poly-Si films.

**Fig. 6.** Nucleation and growth data and fitting for the temperature of 620 °C (**a**) and 630 °C (**b**) using the cylindrical model with  $D=30$  nm (solid line). The dashed line is for homogeneous growth or hemispherical growth.

**Table I.**

Temperature (°C)		605	620	630	652	700
Roughness Layer Thickness (nm)		1.5	1.7	2.2	3.0	3.3
Si Film Composition (%)	c-Si	50.4	53.1	56.5	56.2	58.5
	a-Si	41.7	39.9	32.1	30.6	27.3
	void	7.9	7.0	11.4	13.2	14.2

The parameters are within about 7% error.

**Table II.**

**a.**

Temperature (°C)	620	630	650	700
$\theta$		2.0	2.0	2.0
S	1.0	0.6	0.6	0.6
$\kappa$	2.0	1.4	1.1	1.1

**b.**

SiH <sub>4</sub> Flow Rate (sccm)	10	20	30	50
$\theta$	0.0	2.0	2.0	2.0
S	0.57	0.57	0.6	0.6
$\kappa$	1.0	1.0	1.1	1.1

The parameters are within about 10% error.

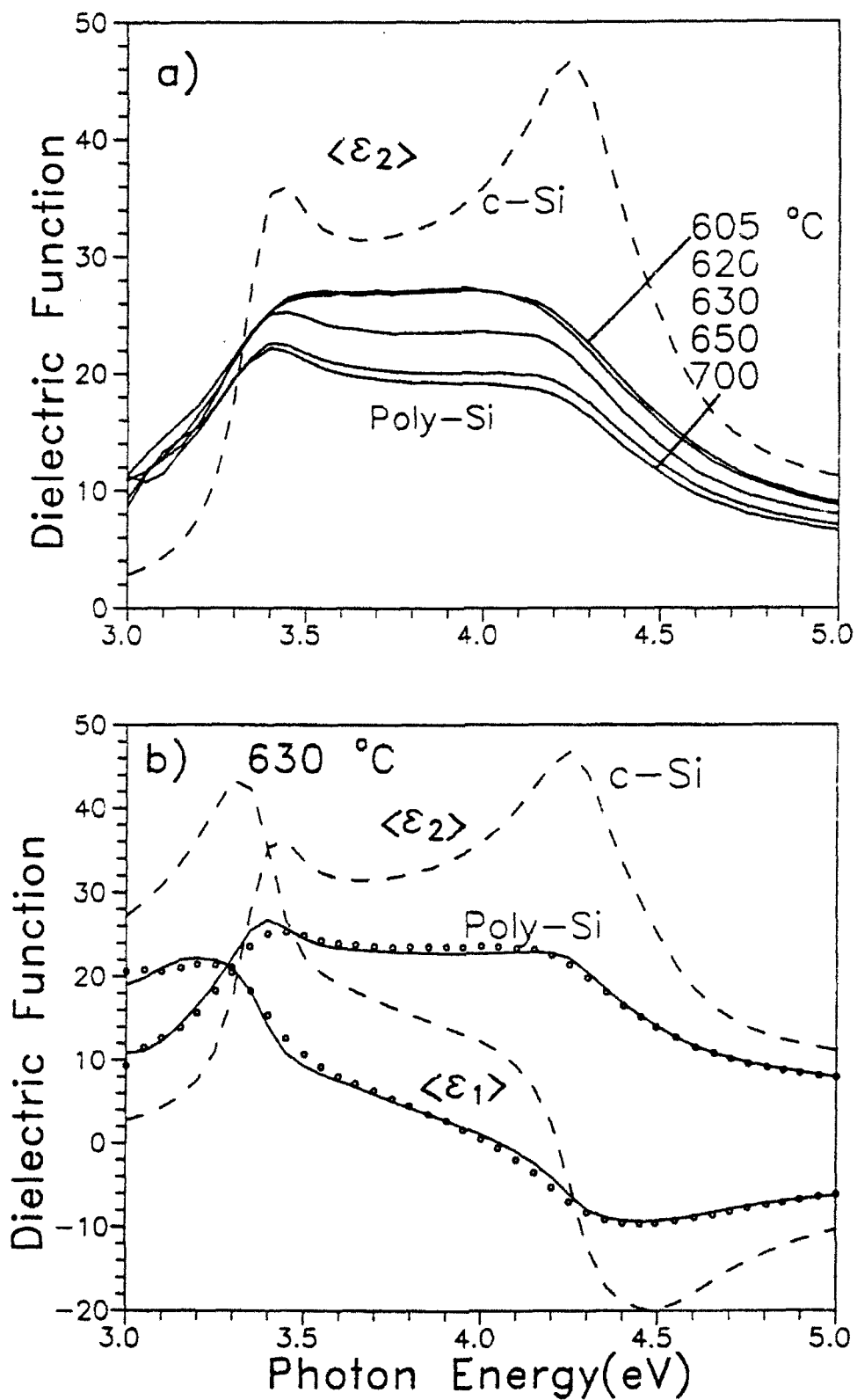


Figure 1

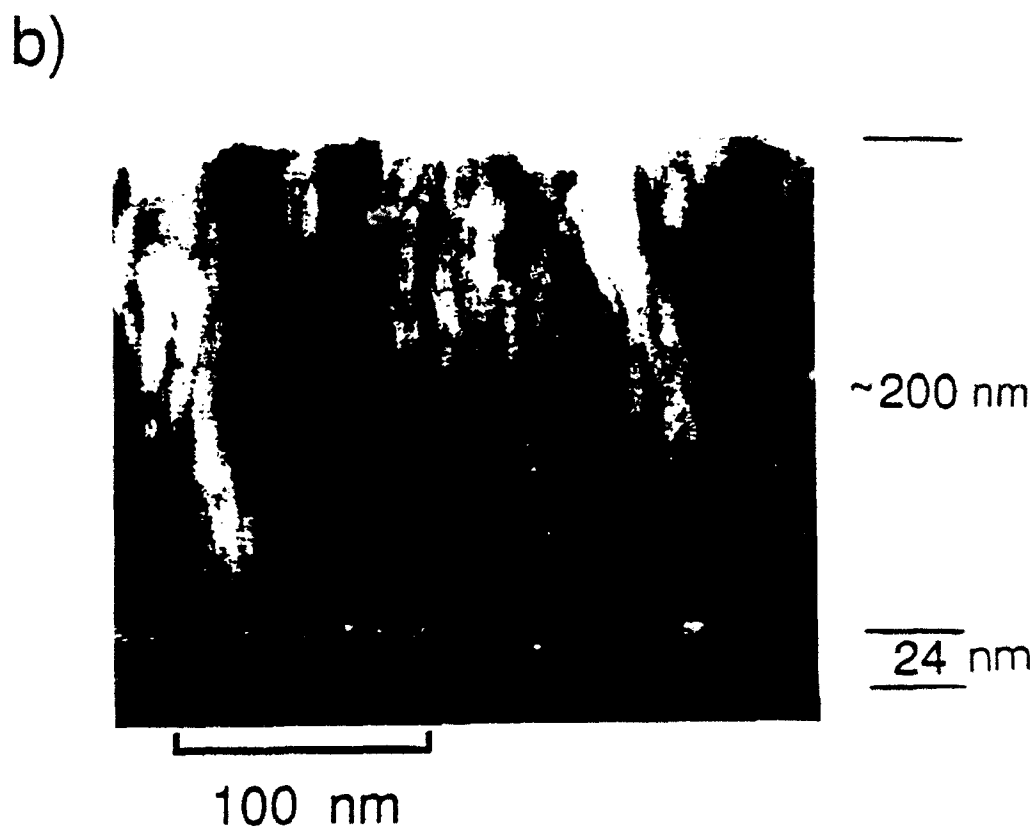
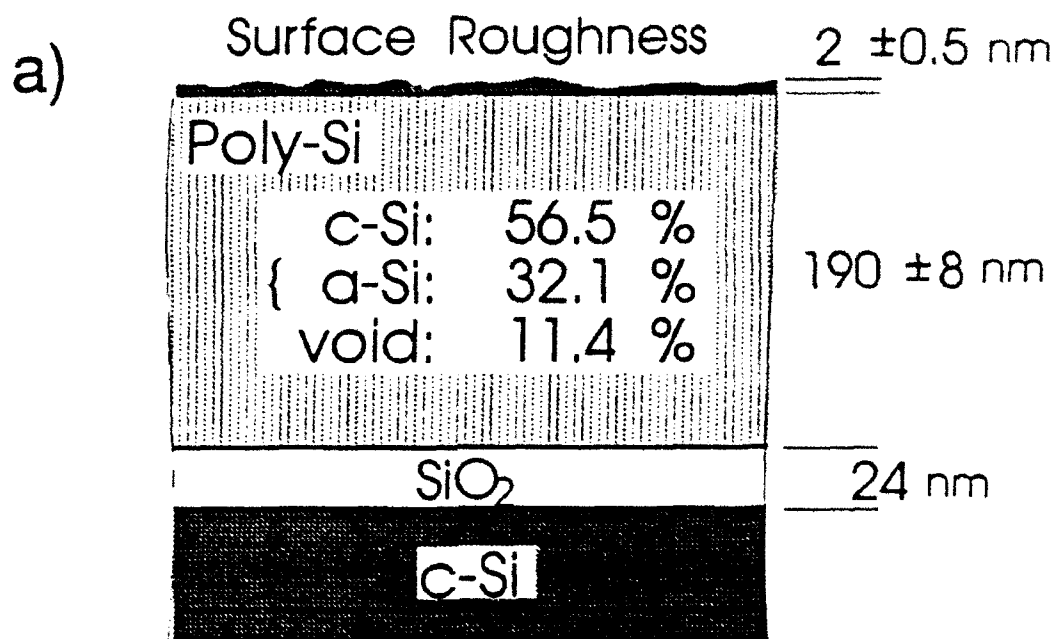


Figure 2

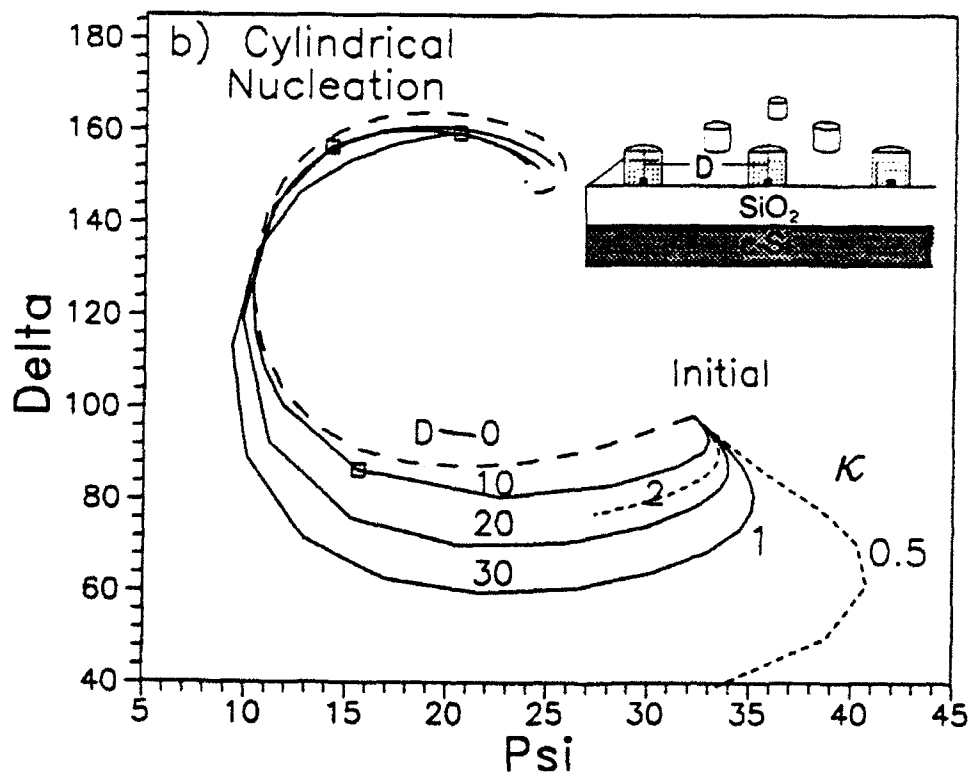
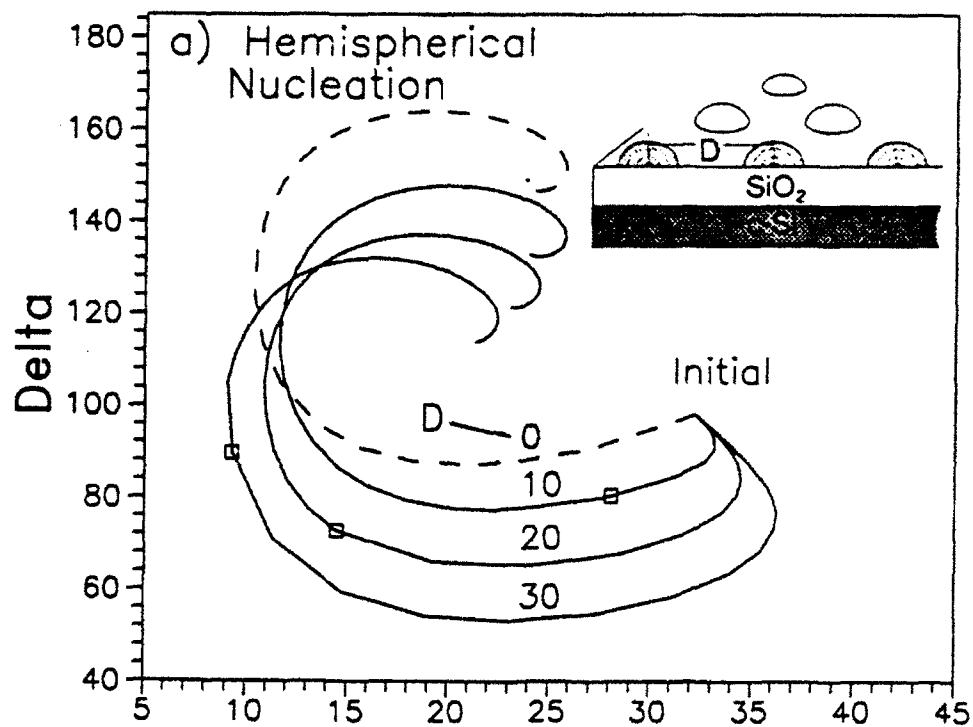


Figure 3

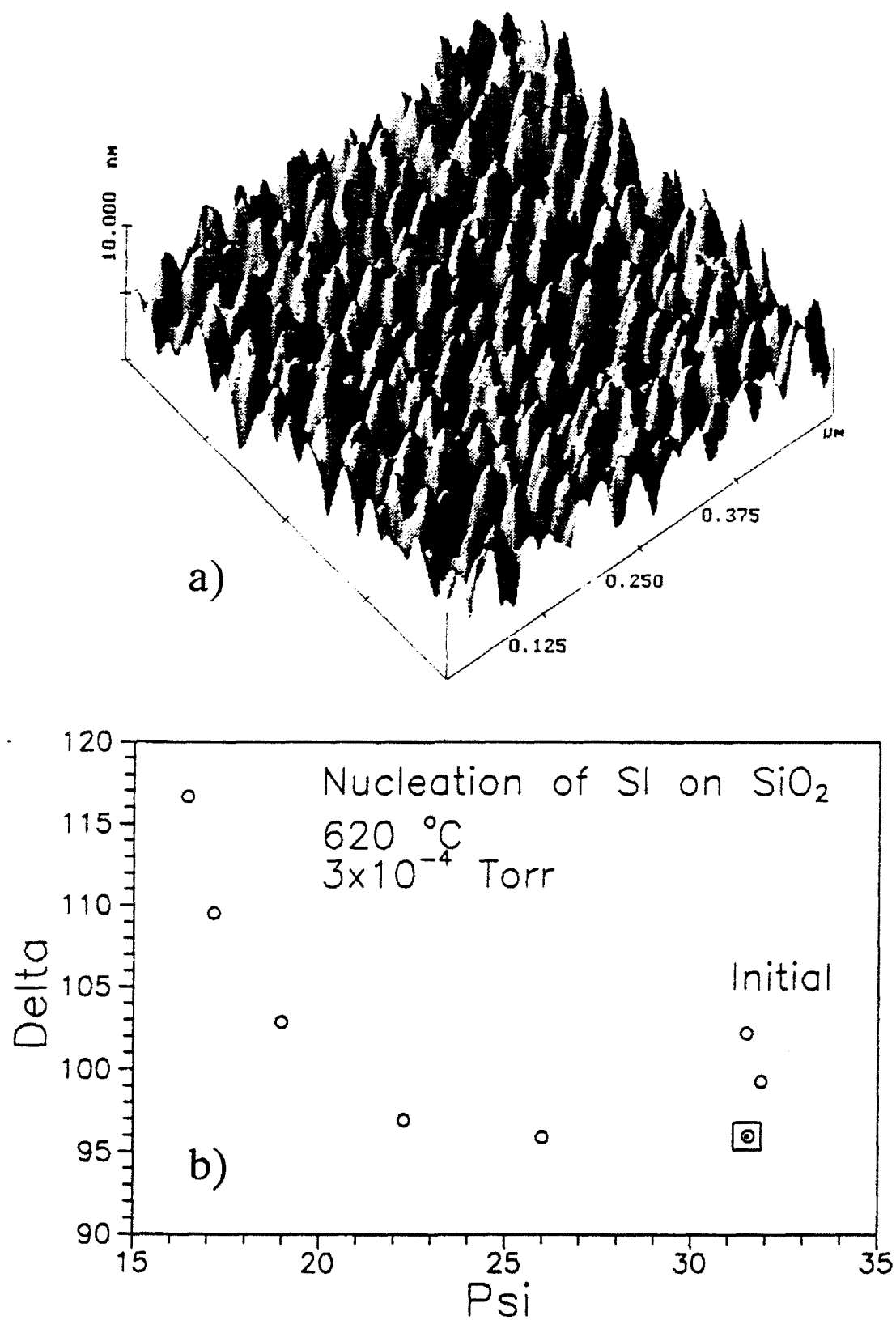


Figure 4



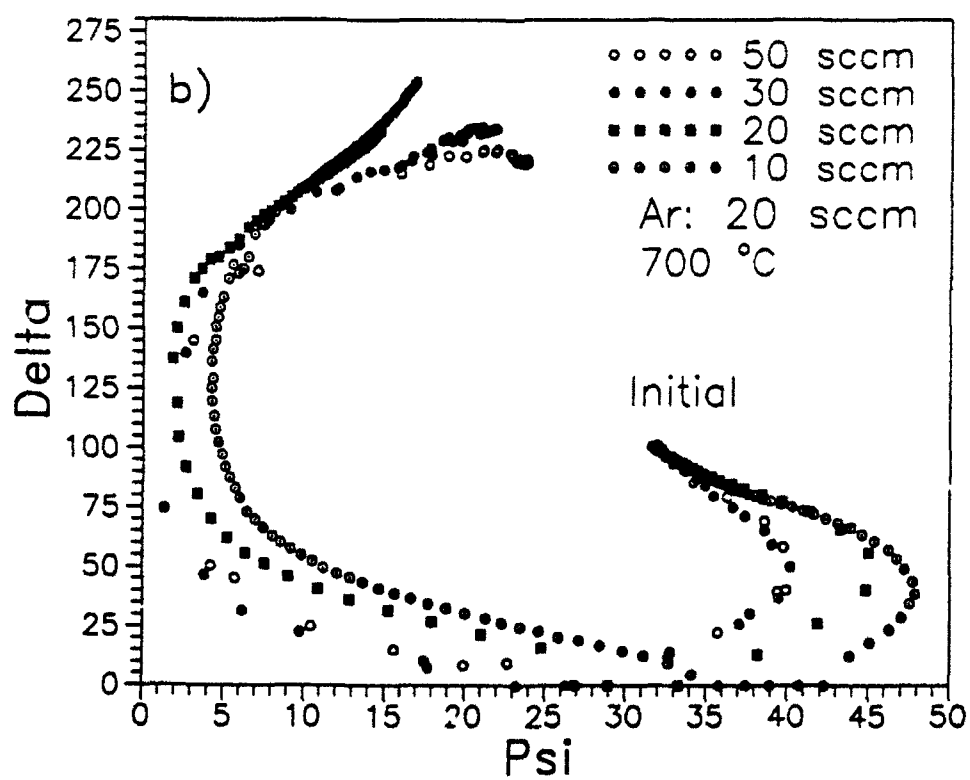
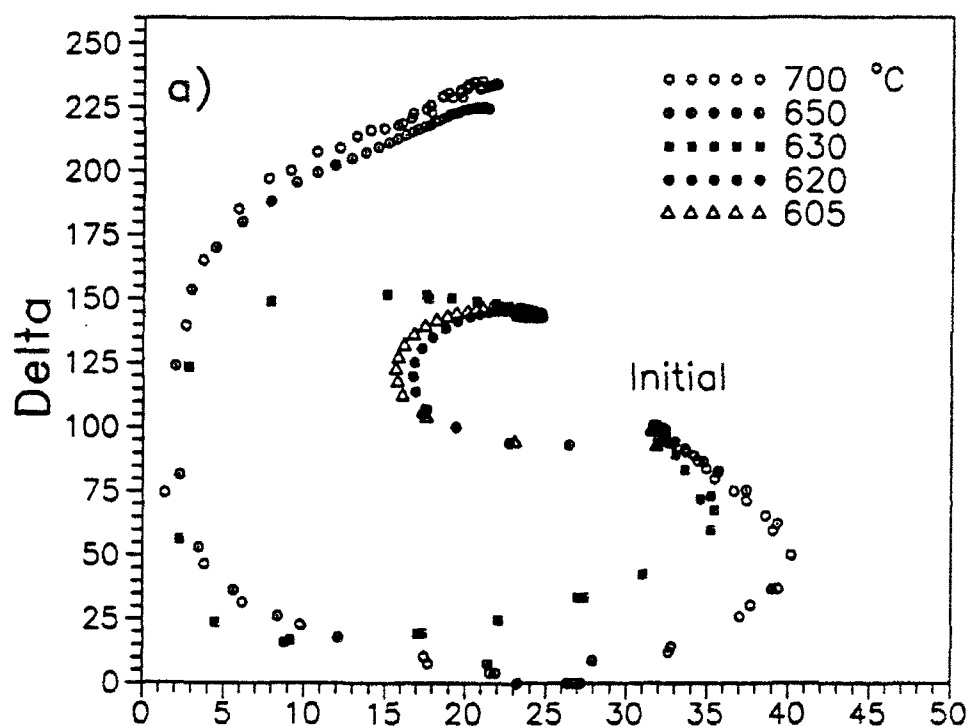


Figure 5

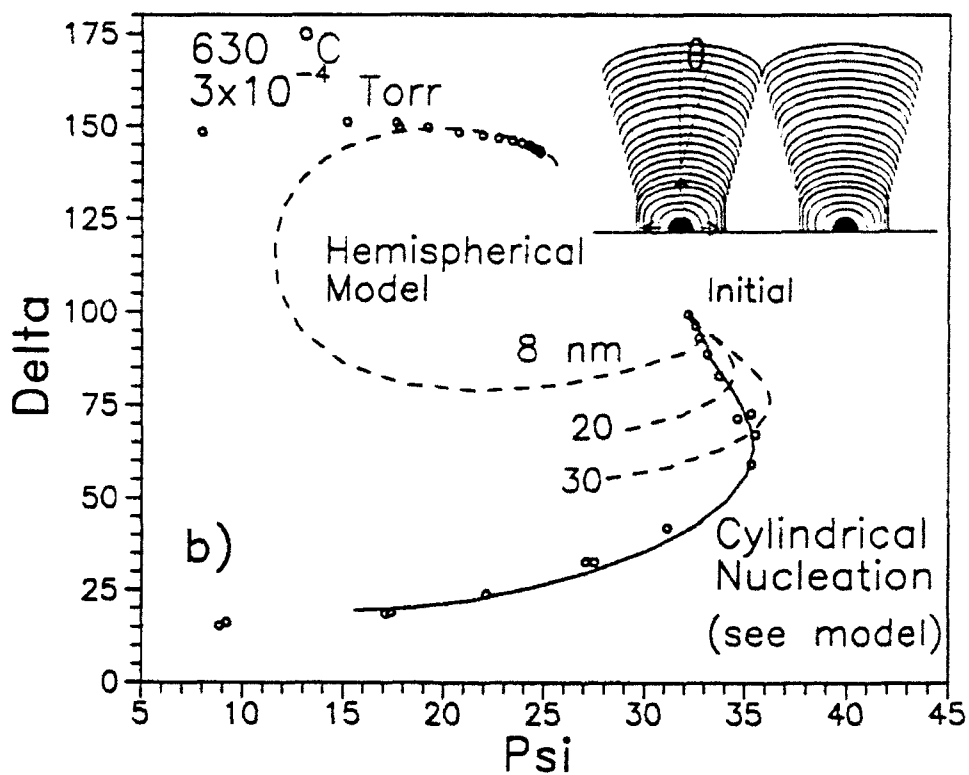
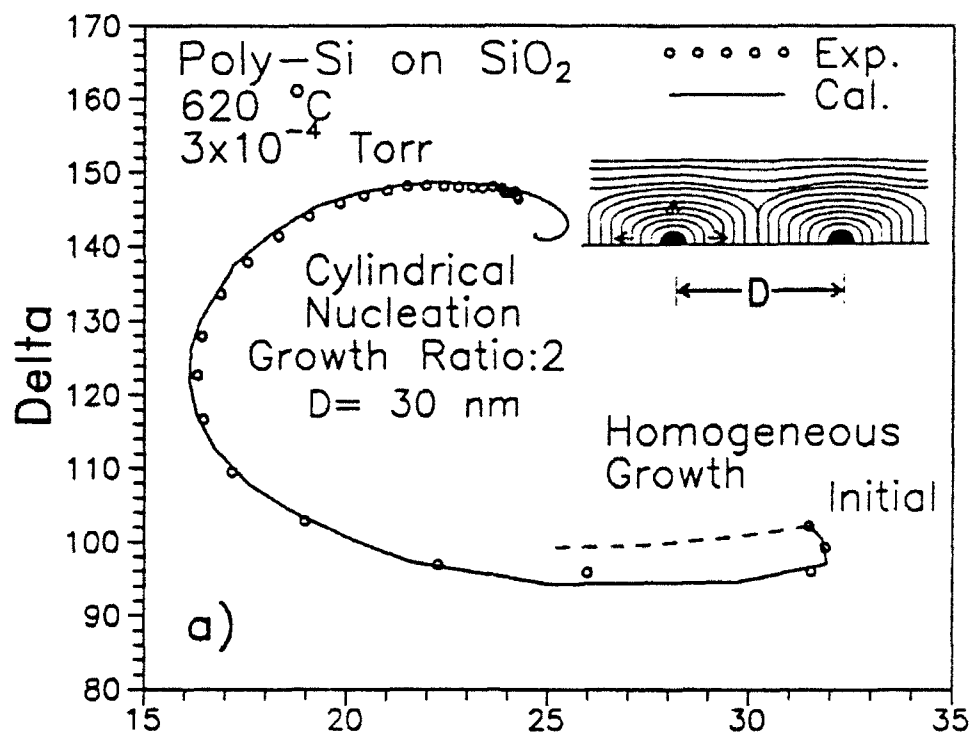


Figure 6